Available online at www.sciencedirect.com
SCIENCE DIRECT®
Journal of Electroanalytical Chemistry 548 (2003) 121–130
Journal of Electroanalytical Chemistry
www.elsevier.com/locate/jelechem

Local reactivity of thin Pd overlayers on Au single crystals

Ata Roudgar, Axel Groß *

Physik-Department T30, Technische Universität München, James-Frank-Str., 85747 Garching, Germany

Received 23 December 2002; received in revised form 11 March 2003; accepted 29 March 2003

Abstract

The local reactivity of thin pseudomorphic Pd overlayers on Au(111) and (100) single crystal surfaces has been studied by periodic density functional theory calculations within the generalized gradient approximation. We have determined the adsorption energies of atomic hydrogen and of CO as a microscopic probe of the reactivity. We demonstrate that both surface strain effects and substrate interaction effects contribute to the modification of the reactivity of the overlayer system. While there is no unique trend in the adsorption energies as a function of the lattice strain, at all considered adsorption sites we find a maximum of the binding energies of both H and CO on two Pd overlayers on Au thus providing a microscopic explanation for recent experiments on the electrochemical reactivity of flat Pd nanoparticles on Au(111). Furthermore, we address the initial stages of Pd deposition on Au.

Keywords: Electronic structure calculations; Thin layer; Chemisorption; Electrocatalysis; Hydrogen evolution; CO; Palladium; Gold

1. Introduction

The catalytic properties of thin metal overlayers deposited on a foreign substrate can be significantly modified with respect to those of the bulk metal [1]. Therefore, a detailed understanding of the underlying microscopic mechanisms responsible for the modification of the reactivity in bimetallic systems is highly desirable. It might lead to the design of better catalysts in both heterogeneous and electro-catalysis [2,3], in particular since bimetallic systems might offer the possibility to tailor the reactivity by preparing specific surface compositions and structures.

In electrochemistry, Pd overlayers deposited on Au single crystal surfaces have been studied in detail as a well-defined model system [4–12]. Due to the relatively small lattice mismatch between Pd and Au of 5%, up to 10 layers of Pd can grow pseudomorphically on Au(100) [13] and up to four Pd layers on Au(111) under electrochemical conditions [6]. In vacuum, on the other hand, rough Pd/Au film growth and alloy formation has been observed [14,15]. Alloy formation on Au(100) [7] and Au(110) [12] has also been observed under electrochemical conditions, which, however, seems to depend on the preparation conditions [16]. Hence experimentally it is not fully clear how many Pd layers grow pseudomorphically on Au single crystals.

As far as the electrocatalytic activity of the Pd/Au overlayer systems is concerned, it has been found that the hydrogen adsorption/desorption [4,9] and the electro-oxidation of small organic molecules such as formaldehyde [9] and formic acid [5] show a strong dependence on the layer thickness of the deposited Pd films. Similarly, small Pd nanoparticles deposited on Au(111) in an electrochemical STM set-up exhibit a significantly higher reactivity than bulk Pd [17].

In order to understand the catalytic activity of overlayer systems, two effects have to be taken into account. In addition to the direct electronic interaction of the pseudomorphic overlayers with the metal substrate, geometric strain effects due to the lattice mismatch can change the reactivity of thin films [18–21]. Although there has been a significant progress in the detailed experimental characterization of electrode surfaces and reactions at electrochemical interfaces [22], still it is not trivial to disentangle these effects in the experiment. In such a case, total energy calculations based on first-principles electronic structure theory can

* Corresponding author. Tel.: +49-89-289-12355; fax: +49-89-289-12296.
E-mail address: agross@ph.tum.de (A. Groß).

0022-0728/03/$ - see front matter
doi:10.1016/S0022-0728(03)00230-4

be very helpful. In recent years they have become an efficient and reliable tool to obtain qualitative and often even quantitative insights into the structure and chemistry of surfaces [23–26].

We have performed periodic density functional theory (DFT) calculations of thin pseudomorphic Pd overlayers on Au(111) and (100) single crystal surfaces in order to contribute to the understanding of the modified reactivity of overlayer systems. As a microscopic probe of the local reactivity we have calculated the adsorption energies of atomic hydrogen and CO on various adsorption sites. Note that one has to be cautious by identifying adsorption energies with reactivity. High catalytic activity usually is the consequence of a compromise between a sufficiently strong interaction in order to lead to, e.g. lower dissociation barriers than in the gas phase with a relatively modest binding strength of the products so that they can desorb again. Still, the interaction strength of molecules with surfaces is often closely correlated with the reactivity for a large class of catalytic reactions, for example via a Brønsted–Evans–Polanyi-type relation [27].

We find that at all considered adsorption sites the binding energies of both H and CO show their maximum on two Pd overlayers. By calculating the adsorption energies on pure strained Pd surfaces, we are able to discriminate between strain and substrate interaction effects. Both effects contribute substantially to the modified reactivity of the overlayer system. Our results thus provide a microscopic explanation for the increased reactivity of small Pd nanoparticles on Au(111) [17]. In addition, we briefly address the initial stages of the Pd deposition on Au in vacuum and at the solid–liquid interface.

A preliminary account of this work has already been given [28]. Here we focus in particular on the electronic factors determining the change in the reactivity which we have carefully analysed. Most of our findings can be rationalized within the d-band model [29,30]. However, additionally second nearest neighbor effects turn out to be important for the overlayer systems. Furthermore, we find that the d-band model is no longer fully appropriate if the coupling between adsorbate and substrate is too strong.

2. Computational method

Self-consistent periodic DFT calculations have been performed using the Vienna ab initio simulation package (VASP) [31]. The exchange-correlation effects have been described within the generalized gradient approximation (GGA) using the Perdew-Wang (PW-91) functional [32]. The ionic cores are represented by ultrasoft pseudopotentials [33] as constructed by Kresse and Hafner [34]. The Kohn–Sham one-electron valence states are expanded in a basis of plane waves with the size of the basis characterized by the maximum kinetic energy, the so-called cutoff energy. It turned out that cutoff energies of 200 eV for hydrogen adsorption and 400 eV for CO adsorption are sufficient in order to obtain converged results.Throughout the study we used the calculated equilibrium lattice constants for bulk Pd and Au, 3.96 and 4.18 Å, respectively, which are in good agreement with the experiment (3.88 and 4.08 Å [35], respectively).

The Pd/Au overlayer structures are modeled by a slab of five layers of Au on which up to three Pd overlayers have been deposited. All layer structures are separated by 14 Å of vacuum. The three bottom layers of the slabs have been kept fixed at their corresponding bulk positions, while all upper layers including the overlayers have been fully relaxed. Although it has been found that the H adsorption process is strongly influenced by the anion of the supporting electrolyte [4], as a first step we have addressed the interaction of hydrogen and CO with Pd overlayers of Au in the absence of any electrolyte. This is the usual approach in the ab initio treatment of molecule–surface interactions of electrochemical interest [36] due to the difficulties of realistically incorporating any electrolyte in electronic structure calculations. However, we have also performed first, still preliminary calculations for the hydrogen adsorption on Pd under the presence of a thin film of water [37]. These calculations indicate that the presence of water weakens the interaction between the metal and the adsorbate, but only by less than 100 meV. Similar results have already been obtained in a DFT study of the deprotonation of acetic acid over Pd(111) in the presence of water molecules [38]. Therefore, the general trends found in our present study should also be relevant for the understanding of the energetics of electrochemical reactions.

The adsorption energies are determined in (2×2) and (1×1) surface unit cells corresponding to coverages of $\Theta = 0.25$ and 1, respectively. The surface Brillouin zone is sampled by a Monkhorst-Pack **k**-point set [39] of $7 \times 7 \times 1$ $(17 \times 17 \times 1)$ for the 2×2 (1×1) unit cell, corresponding to 8 (45) **k**-points in the irreducible Brillouin zone. A Methfessel–Praxton smearing [40] of $\sigma = 0.2$ eV has been used in order to get a faster convergence of the electronic structure calculations. For the analysis of the electronic structure of the (2×2) surface unit cell, we used a finer mesh of $11 \times 11 \times 1$ **k**-points, corresponding to 16 **k**-points in the irreducible Brillouin zone. The hydrogen adsorption energies are determined via

$$E_{\mathrm{ads}} = E_{\mathrm{slab+H}} - \left(E_{\mathrm{slab}} + \frac{1}{2} E_{\mathrm{H_2}}\right), \tag{1}$$

where E_{slab} and $E_{\mathrm{slab+H}}$ are the total energies of the slab

without and with the adsorbed hydrogen. For the hydrogen binding energy E_{H_2} in the gas phase we have taken the calculated GGA value of 4.550 eV. Since CO adsorbs molecularly, its adsorption energy is given by the following equation

$$E_{ads} = E_{slab+CO} - (E_{slab} + E_{CO}) \quad (2)$$

For the CO binding energy E_{CO} in gas phase we have taken the calculated GGA value of 11.438 eV. Note that the energy gain upon adsorption corresponds to a negative adsorption energy. In the following, we will denote by binding energy the negative of the adsorption energy.

3. Results

3.1. Overlayer structure

It is known that under electrochemical conditions Pd films can be grown in a layer-by-layer fashion on both Au(111) [6,8–10] and Au(100) [16] for the first few layers, however, the growth mode including possible alloy formation apparently depends on the preparation conditions [7,16]. In contrast, under ultra-high vacuum conditions the Pd/Au growth mode strongly depends on the temperature, in particular on Au(111). At low temperatures, rough Pd films grow on Au(111), while at room temperature alloy formation takes place [14,15]. The difference in the growth modes between electrochemical and vacuum conditions has been related to the surface structure of the Au(111) surface [8]. In vacuum, Au(111) shows a complex $(23 \times \sqrt{3})$ herringbone reconstruction [15]. This reconstruction is lifted under electrochemical conditions at the positive potentials at which Pd deposition occurs.

In our electronic structure calculations, we cannot treat the herringbone reconstruction of Au(111) due to computational constraints. Still we have tried to address the growth mode of Pd/Au by calculating the adsorption energy of a Pd atom on Pd(111) and unreconstructed Au(111) in a (3×3) surface unit cell corresponding to a coverage of 1/9 in order to avoid any interaction between the adatoms. We found that the Pd adatom is by 0.103 eV less strongly bound to Au than to Pd. Hence the Pd–Pd interaction is stronger than the Pd–Au interaction which explains the fact that Pd films grow in a rough fashion on Au(111) in vacuum. On the other hand, under electrochemical conditions underpotential deposition (upd) of Pd on Au(111) has been found [6,10,16] indicating that the Pd–Pd interaction should be *weaker* than the Pd–Au interaction. This is at variance with our findings. However, the difference of 0.1 eV in the interaction energies is relatively small compared to the cohesive energies of Pd (3.89 eV per atom) and Au (3.81 eV per atom) [41]. It is therefore reasonable to assume that the Pd–Au interaction is modified to a certain extent by the presence of the electrolyte or the adsorption of anions which could reverse the order of the interaction strength. This suggests that it is not the lifting of the Au(111) reconstruction under electrochemical conditions that leads to the layer-by-layer growth of the Pd films but rather the modified Pd–Au interaction strength. It should be further noted that Takahasi et al. [8] and Naohara et al. [9] do not report any underpotential deposition of Pd on Au.

As for Au(100), it is well-known that this surface also reconstructs in a hexagonally close-packed structure. This reconstruction is lifted at positive potentials [42] and upon Pd deposition [7]. Again, we made no attempt to address the Au(100) reconstruction but rather focused on the reactivity of the Pd/Au overlayer systems.

3.2. Adsorption energies

We have calculated the adsorption energies of atomic hydrogen and CO on the high-symmetry adsorption

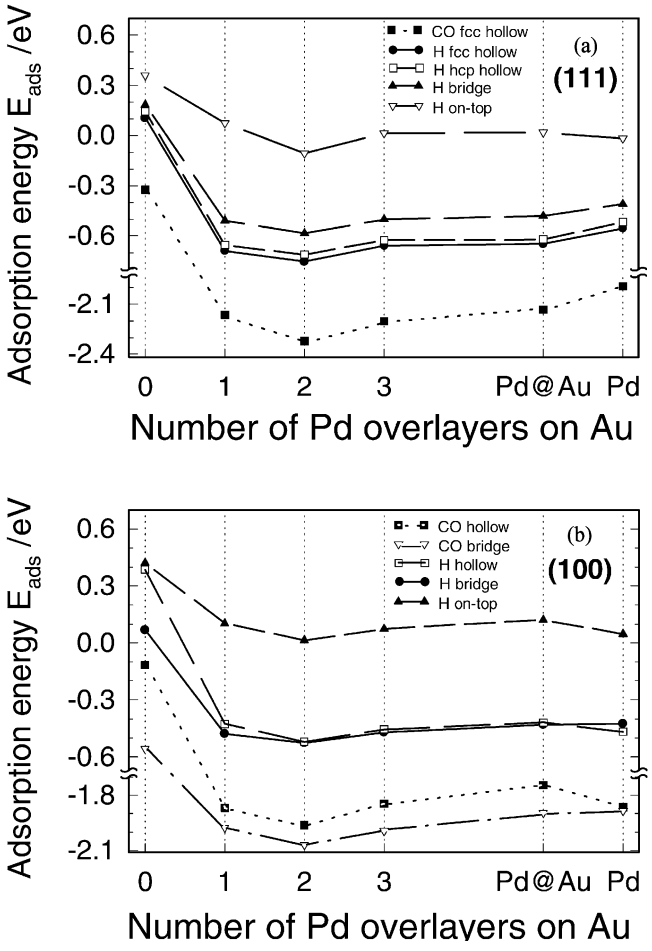

Fig. 1. CO and hydrogen adsorption energies as a function of the number of Pd overlayers on Au for different adsorption sites on the (111) (a) and the (100) surface (b) at a coverage of $\theta = 0.25$. The pure Pd substrates with the lateral lattice constant of Au ($a = 4.18$ Å) and Pd ($a = 3.96$ Å) are labeled by Pd@Au and Pd, respectively.

sites as a function of the number of Pd overlayers on Au(111) and Au(100) (see Fig. 1). The coverage was chosen to be $\theta = 0.25$ which is sufficiently small in order to avoid any significant interaction between the adsorbates. Furthermore, we have determined the adsorption energies on pure Pd slabs where the lateral lattice constants have been kept fixed to the bulk Pd and the bulk Au lattice constant, respectively. The results obtained for the pure Pd surface expanded to the Au lattice constant are denoted by Pd@Au. They correspond to the hypothetical system of infinitely many Pd overlayers grown pseudomorphically on Au. By comparing the results for this system with those for a finite number of Pd overlayers and those for a pure Pd slab with the intrinsic Pd lattice constant, geometrical strain effects can be discriminated from electronic interaction effects with the substrate.

The first striking result evident in Fig. 1 is that CO and H show the same trends in the adsorption energies as a function of the number of Pd overlayers and of the lattice strain despite their different electronic structure and bonding mechanism. The binding energies of both adsorbates on thin Pd/Au overlayers are larger by up to 0.2–0.3 eV than on pure Pd substrates and show their maximum on two Pd overlayers at all considered adsorption sites. At the most densely packed (111) surface, the adsorption energies on three Pd overlayers hardly differ from those on the pure expanded Pd slabs. This means that the electronic effect of the underlying Au substrate only contributes significantly to the reactivity of the first two overlayers. The modified reactivity of the third layer is almost entirely dominated by the geometric effect due to the lattice expansion. For the less densely packed (100) surface, there is still some influence of the Au support up to the third Pd overlayer. This can be understood from the fact that the (100) layers have a smaller spacing than the (111) layers.

As far as the pure strain effects are concerned, we do not find an unique trend. On the Pd(111) surface the binding energies increase upon lattice expansion at the higher-coordinated sites while the top site shows the opposite trend. On the Pd(100) surface, on the other hand, both the fourfold hollow as well as the top site exhibit a weaker binding upon lattice expansion whereas at the bridge site there is a slight increase in the binding strength.

As a reference, we have also calculated the CO and H adsorption energies on Au(111) and Au(100) (see Fig. 1). Note that we did not consider the surface reconstructions of neither Au(111) nor Au(100). Our results confirm the inertness of the Au substrate, i.e. all binding energies are greatly reduced on Au compared to clean Pd and the Pd/Au overlayers.

4. Discussion

4.1. Electronic structure

In order to analyse and understand the trends in the hydrogen adsorption energies, we have utilized the d-band model as proposed by Hammer and Nørskov [30]. In this model, the interaction between an adsorbate and a transition or noble metal is formally split into a contribution arising from the s and p states of the metal and a second contribution coming from the d-band. The interaction with the sp-bands is assumed to lead to an energy renormalization of the adsorbate energy levels. In a simplified expression, the whole d-band is assumed to act as a single electronic level located at ε_d which is chosen to be the center of the d-band. Based on second-order perturbation theory, it can be shown [43,44] that small shifts in the d-band center position of the metal $\delta\varepsilon_d$ are linearly correlated to changes in the chemisorption energies

$$\delta E_{\text{chem}} = \frac{V^2}{|\varepsilon_d - \varepsilon_a|^2}\,\delta\varepsilon_d. \tag{3}$$

Here ε_a is the renormalized adsorbate resonance and V is the d-band coupling matrix element between adsorbate and the surface metal atom.

According to Eq. (3), an upshift of the d-band center is associated with a stronger interaction. A lattice expansion or a reduced coordination leads to a smaller d-bandwidth and, if the d-band is more than half-filled, to an upshift of the d-band due to charge conservation [20,45]. This effect explains for example the higher reactivity of step edge atoms [43,46–49] or expanded surfaces [20].

In Fig. 2 the position of the d-band center is plotted as a function of the number of Pd overlayers on Au(111)

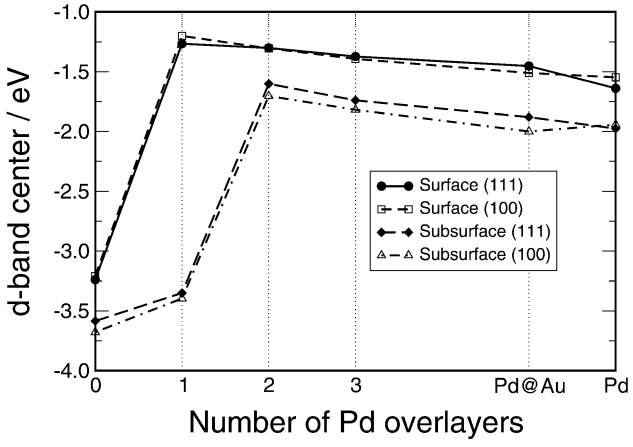

Fig. 2. Position of the local center of the d-band with respect to the Fermi energy as a function of the number of Pd overlayers on Au(111) and on Au(100) for the surface and the subsurface layer. The results for a pure Pd substrate with the lateral lattice constant of Au ($a = 4.18$ Å) and Pd ($a = 3.96$ Å) are labeled by Pd@Au and Pd, respectively.

and Au(100) for the uppermost and the subsurface layer. In general, the (111) and (100) surfaces show rather similar trends. Comparing the data for pure Pd and Pd@Au, it is obvious that expanding the Pd substrate to the Au lattice constant leads to an upshift of the local d-band center at the surface, which is as expected. Interestingly enough, on Pd(100) the d-band center of the subsurface layer shifts down in energy upon lattice expansion. This is a consequence of the relaxation along the surface normal. Upon lateral expansion, the inter-layer spacing decreases, and consequently, the coupling between the layers becomes stronger. For the more open (100) surface this effect even overcompensates the weaker intra-layer coupling. However, in addition to these geometric effects, the electronic interaction of Pd with the underlying Au substrate leads to a further upshift of the Pd d-band. In the following, we will first address the effects induced by pure lattice strain, then focus on the substrate interaction and finally discuss coverage effects.

4.2. Lattice strain effects

Since CO and hydrogen show the same trends in the adsorption energies, we will mainly concentrate on hydrogen adsorption in our analysis of the electronic factors determining the reactivity in the following. The interaction of hydrogen with Pd is well-studied, in particular under vacuum conditions [50–54]. For the unstrained pure Pd surfaces, our results are in agreement with previous calculations, both with respect to hydrogen adsorption [55–57] as well as to CO adsorption [58,59]. DFT calculations have found a surface reactivity increasing with lattice expansion, as far as O and CO adsorption energies and the CO dissociation barrier on Ru(0001) are concerned [20], in agreement with the experiment [18,19]. In our calculations, on the other hand, we do not obtain a unique trend of the adsorption energies as a function of the lattice expansion. While the binding energies at the threefold hollow and the bridge position on the Pd(111) surface increase with lattice expansion, they decrease at the top position of both the (100) and (111) surface and at the fourfold hollow position of Pd(100). This non-uniform behavior is at variance with the statements of the d-band model, which would predict an increase in the adsorption energies at all sites due to the d-band center upshift upon lattice expansion.

First we address the question whether this unexpected behavior could be due to an extension of the adsorbate–substrate bond upon expansion which would result in a weaker interaction. In Table 1 we have listed the adsorption heights and distances to the nearest Pd atoms for all considered hydrogen adsorption sites at the unstrained and strained surfaces. Upon expanding the lateral lattice constant of the Pd(111) surface by 5%, the hydrogen adsorption height at the bridge site is reduced from 0.97 to 0.86 Å and from 0.81 to 0.61 Å at the threefold fcc hollow position. This process is illustrated in Fig. 3; d and d′ are the bond length before and after the expansion, respectively. The downward relaxation of the hydrogen atoms occurs in such a way that the H–Pd distances to the nearest neighbors are kept constant within ± 0.01 Å. We have found the same effect for CO adsorption on Pd(111), where the adsorption height at the fcc hollow position is reduced from 1.30 to 1.19 Å, thus keeping the C–Pd distances to the nearest neighbors of $d = 2.08$ Å constant.

This mechanism can not work any longer at the fourfold hollow position of the (100) surface. There the hydrogen atom sits already rather deep in the first Pd surface layer only 0.32 Å higher than the Pd atoms. Hence it is also directly interacting with the subsurface layer so that it becomes effectively fivefold coordinated. Although the hydrogen atom reduces its height to 0.14 Å upon the lattice expansion and the neighboring Pd atoms also relax towards the hydrogen atom, still the H–Pd bond length increases from 1.99 to 2.06 Å. The reduced H–Pd interaction and the energetic cost of the Pd atom relaxations overcompensate the increase in the reactivity of the expanded surface due to the d-band center upshift. As a result, the fourfold hollow and the bridge site become energetically degenerate.

In the case of CO adsorption at the hollow site, we see a qualitatively similar behavior: upon lattice expansion, the CO binding strength decreases. Although the adsorption height is much larger, 1.05 Å, there is still some direct interaction with the subsurface atom, as the analysis of the LDOS confirms. This interaction is increased upon lattice expansion since the CO distance to the subsurface Pd atom reduces from 3.10 to 2.92 Å. This effectively higher coordination is energetically unfavorable for CO resulting in a weaker binding.

The hydrogen adsorption energies on the on-top positions of Pd(100) and Pd(111) also show the opposite trend upon lattice expansion than expected from the d-band shift. However, here the adsorption height which at this site is the same as the nearest-neighbor distance to the adjacent Pd atom remains basically unchanged upon lattice expansion. Hence bond length effects can not be the source for the unexpected trend in the adsorption energies as a function of lattice strain.

It is important to note that at the top site the hydrogen atom is mainly interacting with the Pd atom directly beneath. Furthermore, the hydrogen 1*s* state only couples to the Pd $d_{3z^2-r^2}$ orbital since all other d orbitals are not rotationally symmetric with respect to the Pd–H bond along the *z*-axis. This means that the H atom at the top site is much more strongly interacting with the single Pd $d_{3z^2-r^2}$ orbital compared to the interaction of the H atom with the Pd d orbitals at the higher coordinated site, as a comparison of the H-

Table 1
Atomic hydrogen adsorption height h and nearest-neighbor distance d_{Pd-H} between hydrogen and Pd on various high-symmetry adsorption sites on Pd(111) and Pd(100) as a function of the lattice strain

	Pd(111)						
Lattice	fcc hollow		hcp hollow		bridge		top
Constant	h	d_{Pd-H}	h	d_{Pd-H}	h	d_{Pd-H}	$h = d_{Pd-H}$
3.96	0.81	1.83	0.73	1.82	0.97	1.73	1.56
4.18	0.61	1.83	0.58	1.83	0.86	1.73	1.56
	Pd(100)						
			fourfold hollow		bridge		top
			h	d_{Pd-H}	h	d_{Pd-H}	$h = d_{Pd-H}$
3.96			0.32	1.99	0.99	1.72	1.56
4.18			0.14	2.06	0.88	1.72	1.55

All distances are given in Å.

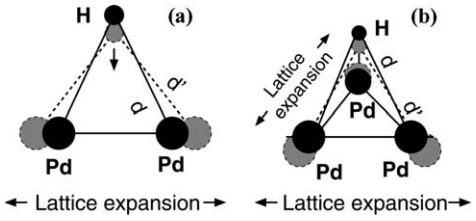

Fig. 3. Schematic sketch of the change of the H adsorbate height upon lattice expansion. (a) Bridge site; (b) threefold hollow site. Upon lattice expansion the hydrogen atoms relax towards the surface so that the optimum H–Pd distance d is kept constant.

adsorption induced LDOS at the fcc site (Fig. 4a) and the top site (Fig. 4b) of Pd(111) confirms. While at the fcc site the Pd d-band LDOS is hardly changed by the presence of the adsorbed hydrogen atom, at the top site there is strong hybridization between the H 1s-derived state and the Pd $d_{3z^2-r^2}$ orbital.

Fig. 4c shows the LDOS for hydrogen adsorption on the top site of the *expanded* Pd(111) surface. As far as clean Pd(111) is concerned, it is obvious that the local d-band is narrower and its center higher than on the unstrained surface which should make it more reactive according to the d-band model. However, the hydrogen induced downshift of the Pd d-band at the unstrained surface is larger by 0.10 eV compared to the expanded surface, as can already be infered from a careful inspection of Fig. 4b and c. The larger H induced d-band downshift at the unstrained surface overcompensates the effect of the higher d-band center at the expanded surface and thus stabilizes the adsorption at the unstrained surface. This analysis shows that the d-band model is only appropriate if the interaction between adsorbate and substrate is not too strong [60]. If there is a strong coupling, then the response of the local d-band to the presence of the adsorbate has to be taken into account in addition to the d-band position in order to understand the reactivity. An equivalent behavior has also been observed in the system H/Cu [61].

4.3. Substrate interaction effects

For Pd pseudomorphic overlayers on Au, the interaction of Pd with the Au substrate leads to a further upshift of the local d-band center of the Pd overlayers, as shown in Fig. 2. In order to understand the reasons for the upshift, we have plotted in Fig. 5 the local d-band density of state for one Pd atom adsorbed per 3×3 surface unit cell on Au(111) and Pd(111), respectively. As already mentioned, Pd atoms are by 0.103 eV less strongly bound to Au than to Pd. This difference is not too large with respect to the cohesive energies of Pd and Au. However, the difference in the local d-band density of state of the Pd atom adsorbed on both surfaces is quite significant.

Au has a deep-lying filled d-band which makes it to an inert noble metal [29]. And indeed, on Au(111) the d-band LDOS of the Pd atom is much narrower and higher in energy than on Pd(111), as Fig. 5 shows. This reflects that there is only a weak coupling between the Pd and the Au d electrons. Thus, the attraction between Pd and Au is mainly mediated by the sp electrons. It also explains the further upshift of the d-band center for the Pd overlayers on Au (see Fig. 2) which contributes to the higher reactivity of the overlayer systems.

On the basis of our findings we thus propose that depositing a reactive metal on an inert metal with a larger lattice constant should in general lead to a higher reactivity of the overlayer since both substrate interaction and strain effects increase the reactivity. Exactly the opposite trend we expect for an overlayer of a less reactive metal deposited on a more reactive metal with a smaller lattice constant, such as, e.g. Pt on Ru [62]. This has in fact been verified in both experiment and theory [21,63]. Shubina and Koper have calculated CO adsorp-

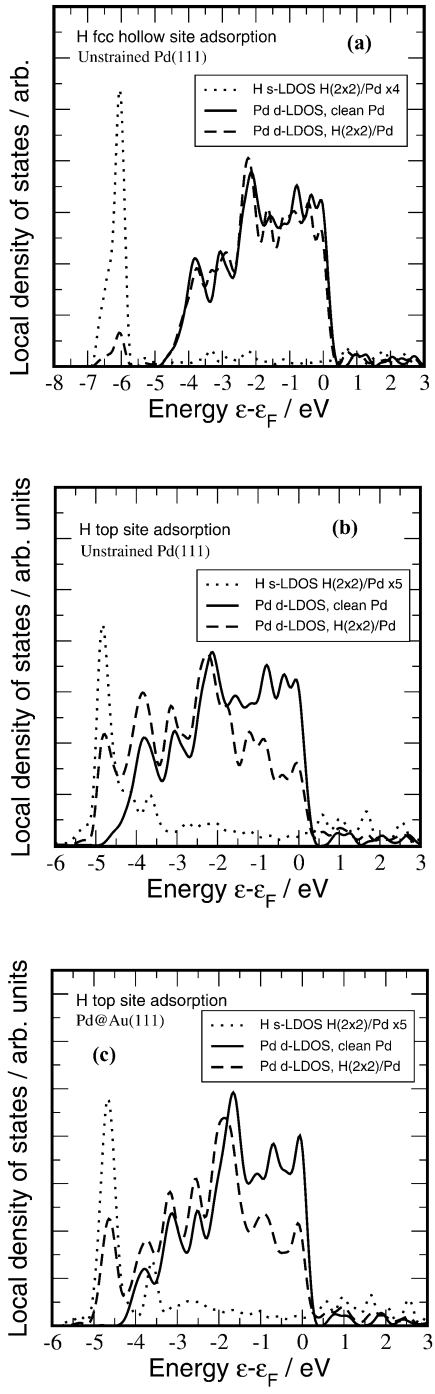

Fig. 4. Local density of states (LDOS) of the hydrogen 1s state and the Pd d-band for atomic hydrogen adsorption on unstrained Pd(111) at the fcc hollow site (a) and the top site (b) and at the top site of strained Pd(111) (c). The hydrogen 1s density of state is multiplied by a factor of 5. The energies are given with respect to the Fermi energy ε_F.

tion energies on a Pt monolayer deposited on a number of different d-band metals [21]. Their results fully confirm our general model proposed above.

However, according to our analysis of the d-band center shifts, one Pd overlayer on Au should show the strongest binding since it has the highest d-band center; nevertheless, the binding energies show a maximum on

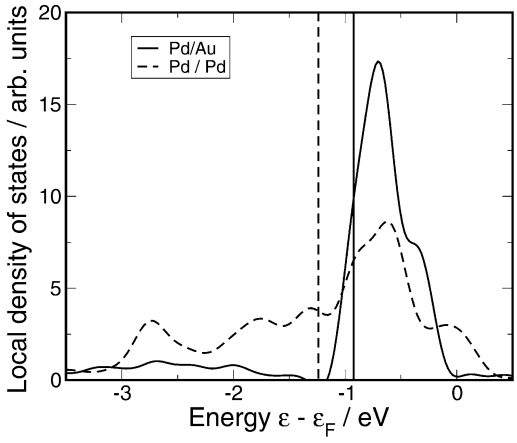

Fig. 5. Local d-band density of states (LDOS) for one Pd atom adsorbed per 3×3 surface unit cell on Au(111) and Pd(111) as a function of the energy. The vertical lines indicate the position of the d-band centers. On Au(111), the d-band LDOS of the Pd atom is much narrower and higher in energy than on Pd(111).

two Pd overlayers on Au (see Fig. 1). Note that the difference in the hydrogen adsorption energies between the fcc and the hcp positions on Pd(111) indicates that the second layer plays an important role for the adsorption because the fcc and hcp sites only differ in the second-nearest neighbors in the subsurface layer. We have therefore analysed the modification of the electronic structure of the subsurface layer upon hydrogen adsorption. Indeed we find that the d-band LDOS of the subsurface layer is still perturbed by the presence of the atomic hydrogen on the surface, even for hydrogen adsorption at the on-top position, as Fig. 6 shows. However, there is hardly any change of the LDOS at the energetic position of the hydrogen 1s adsorbate resonance. This indicates that there is no direct interaction between the adsorbed hydrogen and the second-layer atoms; the interaction is rather mediated indirectly via

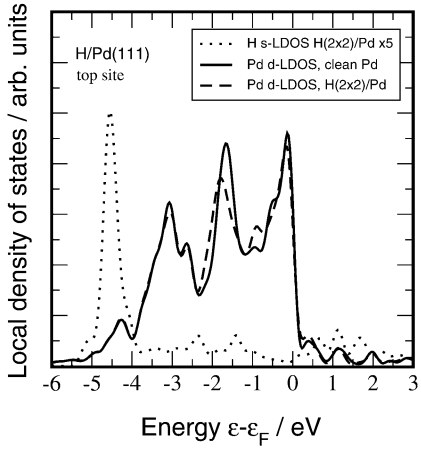

Fig. 6. Local density of states of the hydrogen 1s state and the Pd subsurface d-band for atomic hydrogen adsorption at the top site of two Pd overlayers on Au(111). The hydrogen 1s density of state is multiplied by a factor of 5.

the modification of the electronic structure of the first-layer atoms. In fact, we find that the change in the d-band LDOS of the second layer is mainly caused by those d-orbitals which are participating in the bonding to the first-layer Pd atoms. These findings are all supported by an analysis of the charge density difference induced upon hydrogen adsorption in real space [28].

Having established that there is an significant interaction of the adsorbates with the subsurface layer, we can understand the origin of the maximum in the binding energies for two Pd overlayers. Although the first Pd overlayer should be the most reactive according to the d-band model, there is an indirect coupling to the subsurface layer which consists of gold. Gold as a noble metal is rather unreactive which is reflected by the deep-lying d-band (see Fig. 5). Thus the high reactivity of the first Pd overlayer is overcompensated by the inertness of the Au subsurface layer. For two Pd overlayers, the subsurface layer is more reactive leading to the maximum in the binding energies.

With respect to the substrate interaction, the fourfold hollow site of the (100) surface shows an exceptional behavior in the hydrogen adsorption energies. While for two Pd overlayers the hollow and the bridge site are energetically almost degenerate, on one Pd overlayer the twofold coordinated bridge site becomes favored by 50 meV compared to the fourfold hollow site.

In order to find out the reason for the significant decrease in the binding strength at the fourfold hollow position, it is instructive to analyse the hydrogen adsorption height at both the hollow and the bridge site (Fig. 7). Upon expanding the surface, the adsorption height is reduced both at the bridge and at the hollow position. However, whereas the adsorption height at the bridge site is more or less independent of the number of Pd overlayers on Au, at the hollow site there is a significant increase in the adsorption height when the number of Pd overlayers is reduced from two to one. Recall that at the fourfold hollow position the hydrogen atom is very close to the surface layer so that it is effectively fivefold coordinated. The increase in the adsorption height for one Pd overlayer then indicates that the hydrogen atom is repelled from the subsurface Au atom.

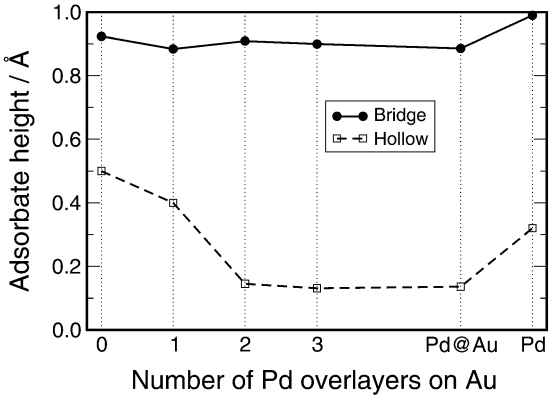

Fig. 7. Hydrogen adsorption height as a function of the number of Pd overlayers at the bridge and fourfold hollow site of the (100) overlayers at a coverage of $\theta = 0.25$.

This conclusion is confirmed by an analysis of the electronic structure which reveals that at the hollow site the adsorbed hydrogen atom is in fact *directly* interacting with the $d_{3z^2-r^2}$ orbital of the Au atom directly beneath in the second layer. Since the d-band of Au is completely filled, this interaction is strongly repulsive. In Table 2 we have collected the relevant distances at this adsorption site. The repulsion between the H and the Au atom is so strong that the Au atom even relaxes downward towards the bulk away from the adsorbed H atom.

Our findings with respect to the hydrogen adsorption energies at the Pd/Au overlayer system are in agreement with recent experiments of the electrochemical hydrogen evolution at small Pd nanoparticles deposited on Au(111) [17]. Pd particles of 0.5, 2.5 and 10 nm height had been investigated. These particles were relatively flat so that they rather corresponded to small nano-islands. The highest reactivity was obtained for the thinnest Pd particles with an height of 0.5 nm which corresponds to two to three Pd layers. According to our calculations, it is the combination of substrate interaction and lattice strain effects that makes thin islands so reactive. For higher pseudomorphic islands, only lattice strain effects are operative. In even higher islands the lattice strain will be relaxed by the formation of dislocations. Thus their reactivity will approach the one of bulk Pd.

4.4. Coverage effects

We have also addressed coverage effects in the hydrogen adsorption energies by repeating the calculations as a function of the number of Pd overlayers on

Table 2
Hydrogen adsorption height h, first interlayer spacing d_{12} and relaxation displacement Δ of the second layer atom just below the adsorbate at the fourfold hollow position for unstrained and strained pure Pd(100) and one Pd overlayer on Au(100)

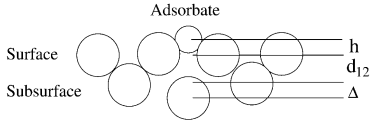

	Pd	Pd@Au	Pd on Au
h	0.32	0.14	0.40
d_{12}	1.98	1.85	1.93
Δ	0.02	0.04	0.13

The geometry is sketched in the figure above the table. All lengths are in Å.

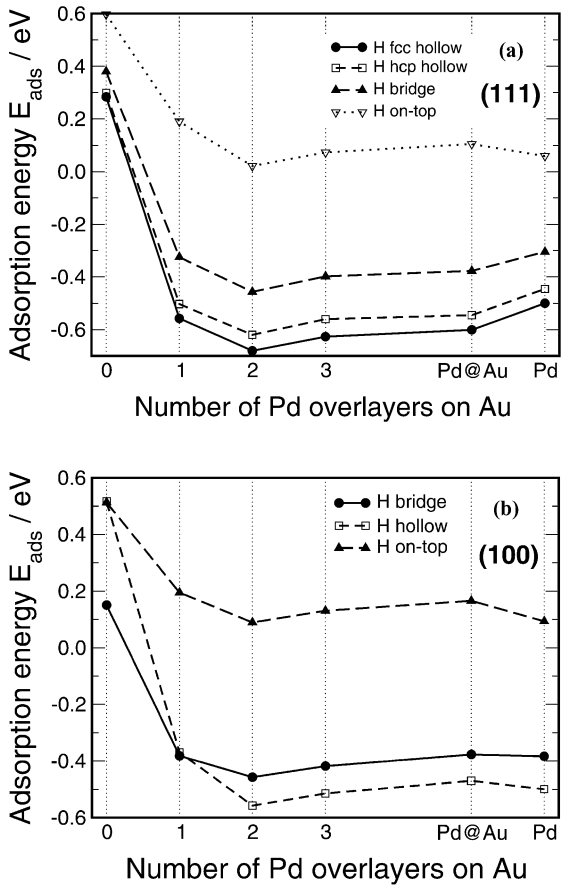

Fig. 8. Hydrogen adsorption energy as a function of the number of Pd overlayers on Au for different adsorption sites on the (111) (a) and the (100) surfaces (b) at a coverage of $\theta = 1$. The pure Pd substrates with the lateral lattice constant of Au ($a = 4.18$ Å) and Pd ($a = 3.96$ Å) are labeled by Pd@Au and Pd, respectively.

Au at a H coverage of $\theta = 1$. The results are shown in Fig. 8a and b for the (111) and (100) surface orientation, respectively. For the (111) orientation, we find basically the same trends in the adsorption energies as a function of strain and the number of Pd overlayers compared to the lower coverage. However, the binding energies at all sites are smaller by 0.04–0.2 eV with respect to the corresponding values at the coverage of $\theta = 0.25$.

At the (100) surface, the hydrogen binding energies at a coverage of $\theta = 1$ are also lowered with respect to the coverage $\theta = 0.25$, but to a smaller extent of only 0.06–0.1 eV. However, the fourfold hollow site again exhibits an exceptional behavior insofar as the binding on pure Pd and on more than one Pd overlayer on Au is in fact slightly *increased* compared to the lower coverage.

These findings can be traced back to an electrostatic interaction between the adsorbates. Note that the adsorption of atomic hydrogen on Pd is associated with an increase in the work function by about 140–390 meV [57,64], depending on the adsorption site. This indicates that there is a charge transfer from the substrate to the adsorbate, creating a dipole layer. The lateral interaction of these dipoles is repulsive. This explains the decrease in the binding energies for higher coverages. It also explains why the effect is slightly larger on the close-packed (111) surface because there the concentration of H atoms is larger.

On the fourfold hollow site, however, the hydrogen atoms are located so deep within the first Pd layer that the electrostatic dipole–dipole repulsion between adjacent hydrogen atoms is effectively screened so that a small net attraction between the hydrogen atoms remains [55,64]. On Au(100) and one Pd overlayer, the H minimum energy adsorption position is further away from the surface (see Fig. 7). Hence, there the direct dipole–dipole interaction is operative leading to the net repulsion.

5. Conclusion

Using density functional theory, we have calculated adsorption energies of atomic hydrogen and CO at the high-symmetry positions of thin pseudomorphic Pd films deposited on Au(111) and Au(100). In general, we find that both the lattice expansion of the pseudomorphic Pd films by 5% as well as the interaction of the Pd films with the Au substrate lead to a higher reactivity of the overlayers. Most of our results can be rationalized by the d-band model, which means that there is a direct correlation between the center of the d-band and the reactivity. However, additionally bond length and second nearest neighbor interaction effects contribute to the reactivity. The indirect interaction of the adsorbates with the inert Au substrate leads to a maximum in the binding energies for two Pd overlayers on Au on all adsorption sites that we considered. Furthermore, we find that the d-band model is no longer fully appropriate in the case of a strong coupling between adsorbate and substrate.

Our results explain the dependence of the reactivity of flat Pd nanoparticles on Au(111) on the particle height found experimentally by using an electrochemical STM set-up [17]. The highest reactivity was obtained for the thinnest Pd particles studied which had a height corresponding to two to three layers. We conclude that their high electrochemical reactivity is a consequence of the combination of substrate interaction and lattice strain effects. Still it should be noted that we have treated perfectly flat surfaces in the absence of any electrolyte. Hence our results are only meaningful as far as general trends are concerned. For example, according to the DFT calculations, Pd is more strongly bound to a Pd(111) substrate by 0.1 eV compared to a Au(111) substrate. This is at variance with the experimentally well-established fact of a upd layer of Pd on Au(111). Our results therefore suggest that the Pd–Au interaction is modified by the presence of an electrolyte.

Acknowledgements

This work has been supported by the Deutsche Forschungsgemeinschaft through the priority programm SPP 1030. Useful discussions with R. Hiesgen, J. Meier, H. Kleine, K.A. Friedrich and U. Stimming are gratefully acknowledged.

References

[1] J.A. Rodriguez, Surf. Sci. Rep. 24 (1996) 223.
[2] F. Zaera, Surf. Sci. 500 (2002) 947.
[3] F. Maroun, F. Ozanam, O.M. Magnussen, R.J. Behm, Science 293 (2002) 1811.
[4] M. Baldauf, D.M. Kolb, Electrochim. Acta 38 (1993) 2145.
[5] M. Baldauf, D.M. Kolb, J. Phys. Chem. 100 (1996) 11375.
[6] L.A. Kibler, M. Kleinert, R. Randler, D.M. Kolb, Surf. Sci. 443 (1999) 19.
[7] L.A. Kibler, M. Kleinert, D.M. Kolb, Surf. Sci. 461 (2000) 155.
[8] M. Takahasi, Y. Hayashi, J. Mizuki, K. Tamura, T. Kondo, H. Naohara, K. Uosaki, Surf. Sci. 461 (2000) 213.
[9] H. Naohara, S. Ye, K. Uosaki, J. Electroanal. Chem. 500 (2001) 435.
[10] M.E. Quayum, S. Ye, K. Uosaki, J. Eletroanal. Chem. 520 (2002) 126.
[11] A.M. El-Aziz, L.A. Kibler, J. Electroanal. Chem. 534 (2002) 107.
[12] L.A. Kibler, M. Kleinert, V. Lazarescu, D.M. Kolb, Surf. Sci. 498 (2002) 175.
[13] C. Liu, S.D. Bader, Phys. Rev. B 44 (1991) 12062.
[14] B.E. Koel, A. Sellidj, M.T. Paffett, Phys. Rev. B 46 (1992) 7846.
[15] C.J. Baddeley, R.M. Ormerod, A.W. Stephenson, R.M. Lambert, J. Phys. Chem. 99 (1995) 5146.
[16] T. Kondo, K. Tamura, M. Takahasi, J. Mizuki, K. Uosaki, Electrochim. Acta 47 (2002) 3075.
[17] J.A. Meier, K.A. Friedrich, U. Stimming, Faraday Discuss. 121 (2002) 365.
[18] M. Gsell, P. Jakob, D. Menzel, Science 280 (1998) 717.
[19] P. Jakob, M. Gsell, D. Menzel, J. Chem. Phys. 114 (2001) 10075.
[20] M. Mavrikakis, B. Hammer, J.K. Nørskov, Phys. Rev. Lett. 81 (1998) 2819.
[21] T.E. Shubina, M.T.M. Koper, Electrochim. Acta 47 (2002) 3621.
[22] D.M. Kolb, Surf. Sci. 500 (2002) 722.
[23] A. Groß, Surf. Sci. Rep. 32 (1998) 291.
[24] A. Groß, Surf. Sci. 500 (2002) 347.
[25] J. Greeley, J.K. Nørskov, M. Mavrikakis, Annu. Rev. Phys. Chem. 53 (2002) 319.
[26] A. Groß, Theoretical Surface Science—A Microscopic Perspective, Springer, Berlin, 2002.
[27] J.K. Nørskov, T. Bligaard, A. Logadottir, S. Bahn, L.B. Hansen, M. Bollinger, H. Bengaard, B. Hammer, Z. Sljivancanin, M. Mavrikakis, Y. Xu, S. Dahl, C.J.H. Jacobsen, J. Catal. 209 (2002) 275.
[28] A. Roudgar, A. Groß, Phys. Rev. B 67 (2003) 033409.
[29] B. Hammer, J.K. Nørskov, Nature 376 (1995) 238.
[30] B. Hammer, J.K. Nørskov, Surf. Sci. 343 (1995) 211.
[31] G. Kresse, J. Furthmüller, Phys. Rev. B 54 (1996) 11169.
[32] J.P. Perdew, J.A. Chevary, S.H. Vosko, K.A. Jackson, M.R. Pederson, D.J. Singh, C. Fiolhais, Phys. Rev. B 46 (1992) 6671.
[33] D. Vanderbilt, Phys. Rev. B 41 (1990) 7892.
[34] G. Kresse, J. Hafner, J. Phys.: Condens. Matter 6 (1994) 8245.
[35] N.W. Ashcroft, N.D. Mermin, Solid State Physics, Saunders College, Philadelphia, 1976.
[36] M.T.M. Koper, R.A. van Santen, Surf. Sci. 422 (1999) 118.
[37] A. Roudgar, A. Groß, to be published.
[38] S.K. Desai, V. Pallassana, M. Neurock, J. Phys. Chem. B 114 (2001) 10954.
[39] H.J. Monkhorst, J.D. Pack, Phys. Rev. B 13 (1976) 5188.
[40] M. Methfessel, A.T. Paxton, Phys. Rev. B 40 (1989) 3616.
[41] C. Kittel, Introduction to Solid State Physics, 6th ed., John Wiley & Sons, New York, 1986.
[42] R.R. Adžić, J.X. Wang, O.M. Magnussen, B.M. Ocko, Langmuir 12 (1996) 513.
[43] B. Hammer, O.H. Nielsen, J.K. Nørskov, Catal. Lett. 46 (1997) 31.
[44] V. Pallassana, M. Neurock, L.B. Hansen, B. Hammer, J.K. Nørskov, Phys. Rev. B 60 (1999) 6146.
[45] A. Ruban, B. Hammer, P. Stoltze, H.L. Skriver, J.K. Nørskov, J. Mol. Catal. A 115 (1997) 421.
[46] B. Hammer, Faraday Discuss. 110 (1998) 323.
[47] B. Hammer, Surf. Sci. 459 (2000) 323.
[48] P.K. Schmidt, K. Christmann, G. Kresse, J. Hafner, M. Lischka, A. Groß, Phys. Rev. Lett. 87 (2001) 096103.
[49] M. Lischka, A. Groß, Phys. Rev. B 65 (2002) 075420.
[50] K.D. Rendulic, G. Anger, A. Winkler, Surf. Sci. 208 (1989) 404.
[51] M. Gostein, G.O. Sitz, J. Chem. Phys. 106 (1997) 7378.
[52] A. Groß, S. Wilke, M. Scheffler, Phys. Rev. Lett. 75 (1995) 2718.
[53] A. Groß, M. Scheffler, Phys. Rev. B 57 (1998) 2493.
[54] A. Groß, M. Scheffler, Phys. Rev. B 61 (2000) 8425.
[55] S. Wilke, D. Hennig, R. Löber, Phys. Rev. B 50 (1994) 2548.
[56] S. Wilke, M. Scheffler, Surf. Sci. 329 (1995) L605.
[57] W. Dong, V. Ledentu, P. Sautet, A. Eichler, J. Hafner, Surf. Sci. 411 (1998) 123.
[58] A. Eichler, J. Hafner, Phys. Rev. B 57 (1998) 10110.
[59] B. Hammer, J. Catal. 199 (2001) 171.
[60] B. Hammer, Y. Morikawa, J.K. Nørskov, Phys. Rev. Lett. 76 (1996) 2141.
[61] S. Sakong, A. Groß, Surf. Sci. 525 (2003) 107.
[62] A. Schlapka, U. Käsberger, D. Menzel, P. Jakob, Surf. Sci. 502 (2002) 129.
[63] A. Schlapka, M. Lischka, A. Groß, P. Jakob, submitted.
[64] S. Wilke, D. Hennig, R. Löber, M. Methfessel, M. Scheffler, Surf. Sci. 307 (1994) 76.